

Aberystwyth University

Estimation of coupling constants of a three-spin chain: a case study of Hamiltonian tomography with nuclear magnetic resonance

Lapasar, Elham Hosseini; Maruyama, Koji; Burgarth, Daniel Klaus; Takui, Takeji; Kondo, Yasushi; Nakahara, Mikio

Published in:
New Journal of Physics

DOI:
[10.1088/1367-2630/14/1/013043](https://doi.org/10.1088/1367-2630/14/1/013043)

Publication date:
2012

Citation for published version (APA):

Lapasar, E. H., Maruyama, K., Burgarth, D. K., Takui, T., Kondo, Y., & Nakahara, M. (2012). Estimation of coupling constants of a three-spin chain: a case study of Hamiltonian tomography with nuclear magnetic resonance. *New Journal of Physics*, 14, [013043]. <https://doi.org/10.1088/1367-2630/14/1/013043>

General rights

Copyright and moral rights for the publications made accessible in the Aberystwyth Research Portal (the Institutional Repository) are retained by the authors and/or other copyright owners and it is a condition of accessing publications that users recognise and abide by the legal requirements associated with these rights.

- Users may download and print one copy of any publication from the Aberystwyth Research Portal for the purpose of private study or research.
- You may not further distribute the material or use it for any profit-making activity or commercial gain
- You may freely distribute the URL identifying the publication in the Aberystwyth Research Portal

Take down policy

If you believe that this document breaches copyright please contact us providing details, and we will remove access to the work immediately and investigate your claim.

tel: +44 1970 62 2400
email: is@aber.ac.uk

Estimation of coupling constants of a three-spin chain: a case study of Hamiltonian tomography with nuclear magnetic resonance

This article has been downloaded from IOPscience. Please scroll down to see the full text article.

2012 New J. Phys. 14 013043

(<http://iopscience.iop.org/1367-2630/14/1/013043>)

View [the table of contents for this issue](#), or go to the [journal homepage](#) for more

Download details:

IP Address: 144.124.50.88

The article was downloaded on 06/02/2012 at 11:03

Please note that [terms and conditions apply](#).

Estimation of coupling constants of a three-spin chain: a case study of Hamiltonian tomography with nuclear magnetic resonance

Elham Hosseini Lapasar^{1,5}, Koji Maruyama², Daniel Burgarth³, Takeji Takui², Yasushi Kondo^{1,4} and Mikio Nakahara^{1,4}

¹ Research Center for Quantum Computing, Interdisciplinary Graduate School of Science and Engineering, Kinki University, 3-4-1 Kowakae, Higashi-Osaka 577-8502, Japan

² Department of Chemistry and Materials Science, Osaka City University, Sumiyoshi, Osaka 558-8585, Japan

³ Institute of Mathematics and Physics, Aberystwyth University, Aberystwyth SY23 3BZ, UK

⁴ Department of Physics, Kinki University, 3-4-1 Kowakae, Higashi-Osaka 577-8502, Japan

E-mail: takui@sci.osaka-cu.ac.jp, daniel@burgarth.de, maruyama@sci.osaka-cu.ac.jp, hosseini@alice.math.kindai.ac.jp, ykondo@kindai.ac.jp and nakahara@math.kindai.ac.jp

New Journal of Physics **14** (2012) 013043 (15pp)

Received 5 November 2011

Published 23 January 2012

Online at <http://www.njp.org/>

doi:10.1088/1367-2630/14/1/013043

Abstract. It has been shown that inter-spin interaction strengths in a spin-1/2 chain can be evaluated by accessing one of the edge spins only. We demonstrate this experimentally for the simplest case, a three-spin chain, with the nuclear magnetic resonance technique. The three spins in the chain interact through nearest-neighbor Ising interactions under site-dependent transverse fields. The employed molecule is an alanine containing three ¹³C nuclei, each of which has spin-1/2.

⁵ Author to whom any correspondence should be addressed.

Contents

1. Introduction	2
2. Theory	3
3. Experiment	5
3.1. Sample and spectrometer	5
3.2. Transverse field calibration	6
3.3. Results	7
4. Estimation of coupling constants	9
4.1. Case 1: $\omega_{11} \neq 0$	11
4.2. Case 2: $\omega_{11} = 0$	12
4.3. Estimation	12
5. Summary	14
Acknowledgments	15
References	15

1. Introduction

Fabricating a quantum system that would perfectly function as we desire is very challenging. Even with the most advanced nanotechnology, it is still difficult to build a structure that would have the exact values of system parameters to make it work as we initially designed. This gives rise to the crucial necessity of system identification. In the context of quantum control, the system identification primarily refers to the identification of the system Hamiltonian, also known as Hamiltonian tomography.

Yet, it is in general formidably hard to estimate the Hamiltonian: the number of necessary initial settings and measurements grows exponentially as the system size becomes larger. To make the problem of Hamiltonian estimation more feasible, various schemes for reducing the complexity and/or minimizing the effect of physical noise have recently been studied quite intensively. Examples are indirect, but efficient, schemes of Hamiltonian tomography of spin systems under limited access [1–5] and also an application of (classical) compressed sensing to the quantum setting [6, 7] that greatly reduces the overall complexity.

In the case of nuclear magnetic resonance (NMR), the interactions among spins in a molecule are usually determined by measuring all spins at once. But what if we are allowed to access only a single spin to reconstruct the whole Hamiltonian as in the above examples? In this paper, we report such an indirect Hamiltonian tomography of a three-spin system with NMR as a minimum model. In the molecule, the spins effectively form a one-dimensional (1D) chain with nearest-neighbor interactions, which are of the Ising type. We attempt to estimate the coupling constants by accessing solely the end spin pretending that we had no knowledge about the interactions in advance. Then, we will make a comparison between the estimated coupling constants and the known values determined by standard methods.

We emphasize that the method used here is different from that presented in [5, 8], where the coupling constants are estimated from the energy eigenvalues found from the spectral peaks, which are evaluated from long time evolution of the spin at one end of the chain. In contrast, in the present work we estimate the coupling constants by fitting the time domain data without making use of the spectra. The materials presented in this paper therefore provide the first step

toward the full verification of the scheme discussed in [5, 8]. While nonlinear least-square data fitting is not computationally efficient for large systems, we find that it is very suitable for the three-spin chain and much more robust against relaxation than the method discussed in [5, 8]. Our finding thus paves the way for indirect estimation of a Hamiltonian of a small-scale noisy system, where direct methods are not applicable. In such circumstances, it is impossible to obtain data over longer time periods, which is fundamental for obtaining sharp spectral peaks.

2. Theory

In this section, we review how to estimate the spin–spin interaction strengths in a three-spin Ising chain with site-dependent transverse fields. The model in our mind is a homonucleus molecule with three spins, such as alanine with three ^{13}C nuclei. We may use liquid-state NMR to control and measure the spins.

The initial state is, thus, a thermal state

$$\rho_{\text{th}}(T) = \frac{e^{-H_0/k_B T}}{\text{Tr}[e^{-H_0/k_B T}]}, \quad (1)$$

where

$$H_0 = -\omega_0 (I_z^1 + I_z^2 + I_z^3) \quad \text{with} \quad I_k^1 = \frac{\sigma_k}{2} \otimes I \otimes I, \quad I_k^2 = I \otimes \frac{\sigma_k}{2} \otimes I, \quad I_k^3 = I \otimes I \otimes \frac{\sigma_k}{2}.$$

Here T is the temperature, ω_0 is the common Larmor frequency of the spins and σ_k is the k th component of the Pauli matrices. We drop the interaction terms among spins and chemical shifts of the spins temporarily since they are small enough compared with ω_0 . We note that equation (1) is defined in the laboratory frame.

A weakly coupled system develops according to the Hamiltonian

$$\mathcal{H} = \omega_{11} I_x^1 + \omega_{12} I_x^2 + \omega_{13} I_x^3 + J_{12} I_z^1 I_z^2 + J_{23} I_z^2 I_z^3. \quad (2)$$

Here, ω_{1i} and J_{ij} characterize the transverse field of spin i and the coupling constant between spins i and j , respectively. We note that the Hamiltonian (2) is described in the rotating frames fixed to each spin.

Now we evaluate the dynamics of spin-1

$$M_k(t) \equiv \langle I_k^1(t) \rangle = \text{Tr}[\rho(t) I_k^1], \quad (3)$$

where $k \in \{x, y, z\}$ and $\rho(t)$ is the density matrix of the system at time t . In an ideal situation without relaxation, the time development of the density matrix is unitary and $\rho(t)$ takes the form

$$\rho(t) = (e^{-i\mathcal{H}t}) \rho_{\text{th}}(T) (e^{-i\mathcal{H}t})^\dagger. \quad (4)$$

The dynamics of spin-1 without relaxation and transverse field inhomogeneity is calculated with equation (4) and the result is shown in figure 1 when $\omega_{1i}/(2\pi) = 27$ Hz for all $i = 1, 2, 3$. The coupling constants $J_{12}/(2\pi) = 53.8$ Hz and $J_{23}/(2\pi) = 34.8$ Hz are taken from [9] as an example. It is clear that figure 1 is far from reality, since relaxation and transverse field inhomogeneity effects are not considered: compare figure 1 with actual experimental results given in figure 3.

We first incorporate the effect of transverse relaxation (the T_2 -process) via the operator sum representation $\varepsilon(\rho) = \sum_{j=0}^3 E_j^\dagger \rho E_j$ where $\sum_{j=0}^3 E_j^\dagger E_j = I$ [10, 11]. In our numerical calculation we divided the time interval $[0, T]$, $T = 0.6$ s, into 600 small intervals with the

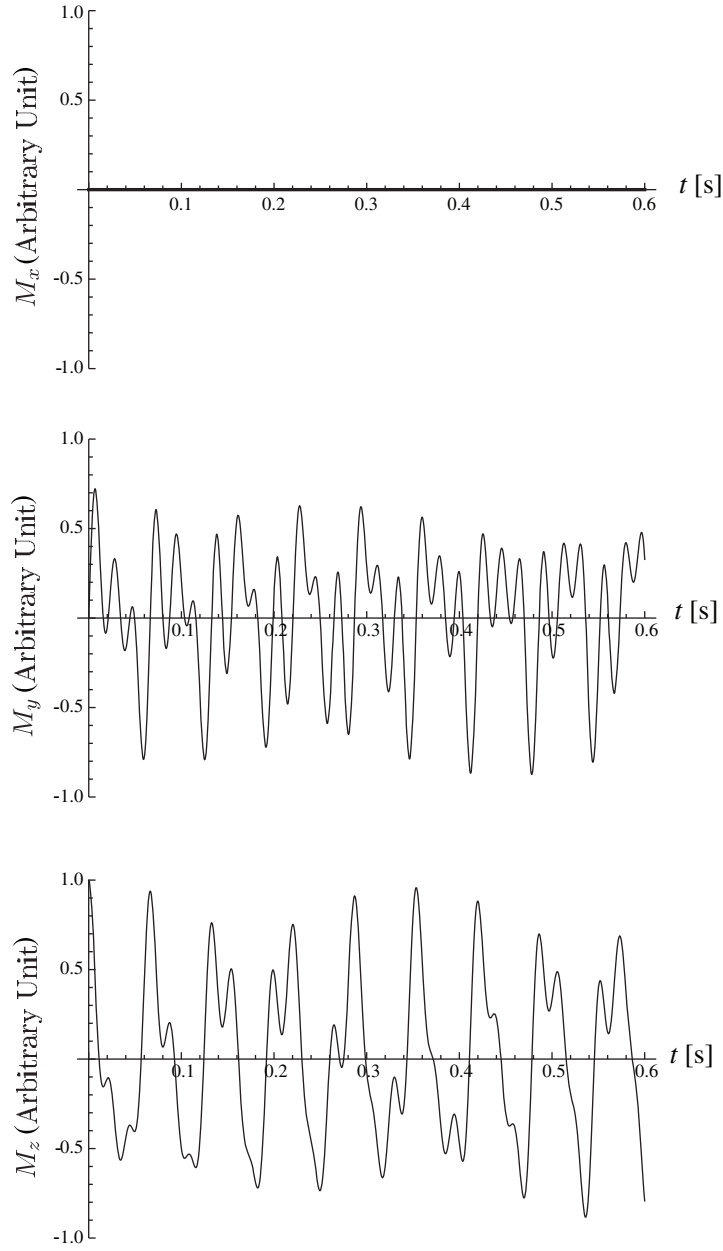


Figure 1. Ideal dynamics of the expectation values $M_k(t)$ ($k = x, y, z$) of spin-1 when the initial state is a thermal state. Parameters $\omega_{1i}/(2\pi) = 27$ Hz, $J_{12}/(2\pi) = 53.8$ Hz, and $J_{23}/(2\pi) = 34.8$ Hz are used in equation (2).

length $\Delta t = 0.001$ s and obtained the density matrix at time $(n+1)\Delta t$ in the presence of relaxation recursively as

$$\rho((n+1)\Delta t) = e^{-i\mathcal{H}\Delta t} \left(\sum_j E_j \rho(n\Delta t) E_j^\dagger \right) e^{-i\mathcal{H}\Delta t^\dagger}, \quad (5)$$

where the error operators for the T_2 -process take the standard form

$$\begin{aligned} E_0 &= \sqrt{\lambda_0} I, \\ E_i &= \sqrt{1 - \lambda_i} (2I_z^i) \quad (i = 1, 2, 3), \end{aligned} \quad (6)$$

with

$$\begin{aligned} \lambda_0 &= \frac{1}{2} \left(-1 + e^{-\Delta t/T_2(1)} + e^{-\Delta t/T_2(2)} + e^{-\Delta t/T_2(3)} \right), \\ \lambda_i &= \frac{1}{2} \left(1 + e^{-\Delta t/T_2(i)} \right) \quad (i = 1, 2, 3), \end{aligned} \quad (7)$$

where $T_2(i)$ is the transverse relaxation time of the i th spin. We confirmed that choosing a smaller interval, $\Delta t = 0.0001$ s, does not change the results.

We ignore the longitudinal relaxation (the T_1 -process) since T_1 for any spin turns out to be much longer than any other characteristic time, such as data acquisition time and $T_2(i)$.

Finally, we take into account the inhomogeneity of the transverse fields $\omega_{1i}(x)$ as a function of position x . We assume that the inhomogeneity has the Gaussian distribution

$$P(\omega_{1i}(x)) = \frac{1}{\sqrt{2\pi}\sigma} \exp \left[-\frac{(\omega_{1i}(x) - \omega_{1i})^2}{2\sigma^2} \right] \quad (8)$$

with variance σ to be determined later.

The system of interest has nine parameters in total, i.e. ω_{1i} , $T_2(i)$, σ , J_{12} and J_{23} . Here we assume that ω_{1i} are known since their controls are in our hands. The field inhomogeneity parameter σ can be fixed as we will discuss later. The relaxation time $T_2(1)$ of spin-1 can be measured directly since it is assumed that we have access to this spin. Eventually, we are left with four unknown parameters ($T_2(2)$, $T_2(3)$, J_{12} , J_{23}) to be estimated. Note, however, that $T_2(2)$ and $T_2(3)$ are expected to influence the short-time dynamics of spin-1 only weakly. This is because it takes time of the order of $T_2(2)$ and $T_2(3)$ for the relaxation of spins 2 and 3 to affect the dynamics of spin-1.

This statement is subsequently justified numerically. Since the dynamics of spin-1 is insensitive to $T_2(2)$ and $T_2(3)$, we may freely employ $T_2(2)$ and $T_2(3)$ measured with the standard NMR technique [9] in the following analysis. Alternatively, we may take $T_2(2) = T_2(3) = \infty$ without changing the estimated coupling constants J_{12} and J_{23} drastically.

Now we are left with two unknown parameters J_{12} and J_{23} , which are to be fixed by fitting the dynamics of spin-1, as a function of J_{12} and J_{23} , with the experimental data.

3. Experiment

We employ a linearly aligned three-spin molecule for demonstrating a Hamiltonian tomography through an edge spin. Our task is to determine the scalar coupling constants J_{12} between spins 1 and 2 and J_{23} between spins 2 and 3 by measuring only spin-1.

3.1. Sample and spectrometer

We demonstrate the Hamiltonian tomography of a spin system with NMR. We employ a Jeol ECA-500 NMR spectrometer⁶, whose hydrogen Larmor frequency is approximately 500 MHz.

⁶ <http://www.jeol.com/>

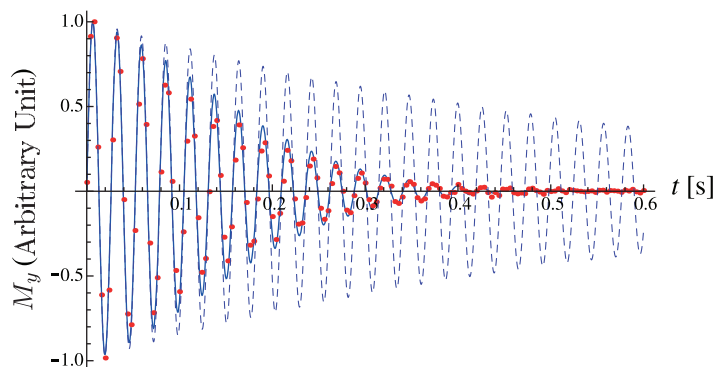


Figure 2. Calibration of the strength and inhomogeneity of transverse field. Experimental results with a setting given in the text are shown by red dots. The dashed line shows the numerical result in which only the effect of relaxation is taken into account, while the solid line is the result in which both relaxation and inhomogeneity of the transverse field are considered.

We apply weak rf fields to generate transverse fields in the rotating frame of each spin. Their strengths are characterized by ω_{1i} .

A 0.3 ml, 0.78 M sample of ^{13}C -labeled L-alanine (98% purity, Cambridge Isotope) solved in D_2O , capsulated in a susceptibility matched NMR test tube (BMS-005J, Shigemi, Tokyo, Japan), is used. Three ^{13}C atoms are linearly aligned in L-alanine. We label the carboxyl carbon spin-1, the α carbon spin-2 and the methyl carbon spin-3.

The scalar coupling constants are estimated from the spectrum obtained by Fourier transforming the free induction decay signal after a hard $\pi/2$ -pulse is applied for readout [9]. Here, protons are decoupled using a standard heteronucleus decoupling technique (WALTZ-16) [12]. The information extracted from the spectrum is summarized as follows. The Larmor frequency differences are $(\omega_{02} - \omega_{01})/2\pi = 15.8 \text{ kHz}$ and $(\omega_{03} - \omega_{02})/2\pi = 4.4 \text{ kHz}$, where ω_{0i} denotes the Larmor frequency of spin i for which the chemical shift is considered. Large differences in the Larmor frequencies compared with the scalar coupling constants guarantee the condition of the weak coupling limit, which is assumed in introducing the Hamiltonian (2). The scalar coupling constant J_{13} between spins 1 and 3 is of the order of 1 Hz [13], which is much smaller compared to J_{12} and J_{23} , and hence we can safely ignore it in our analysis. As a result, the Hamiltonian of the alanine molecule is well approximated by equation (2). Measured relaxation times are $T_1(1) = 15.5 \text{ s}$, $T_1(2) = 1.4 \text{ s}$, $T_1(3) = 0.9 \text{ s}$ and $T_2(1) = 0.45 \text{ s}$, $T_2(2) = 0.23 \text{ s}$, $T_2(3) = 0.63 \text{ s}$, where the argument labels the spin. The spin-2 has the shortest T_2 . In view of the fact that our data acquisition time to estimate the Hamiltonian is much shorter than any of $T_1(i)$, we ignore the effect of T_1 from now on. In contrast, we fully take into account the effect of $T_2(i)$ with equation (5) in our numerical calculations.

3.2. Transverse field calibration

We measure the dynamics of spin-1 in the presence of ω_{11} only, while other ω_{1i} ($i = 2, 3$) are set to 0, as shown in figure 2. The data were acquired every 0.004 s for $0 \leq t \leq 0.6 \text{ s}$. The periodicity provides the information on the strength of the transverse field, $\omega_{11}/(2\pi) = 27 \text{ Hz}$, while the decay rate is determined by the relaxation and the field inhomogeneity. We find that

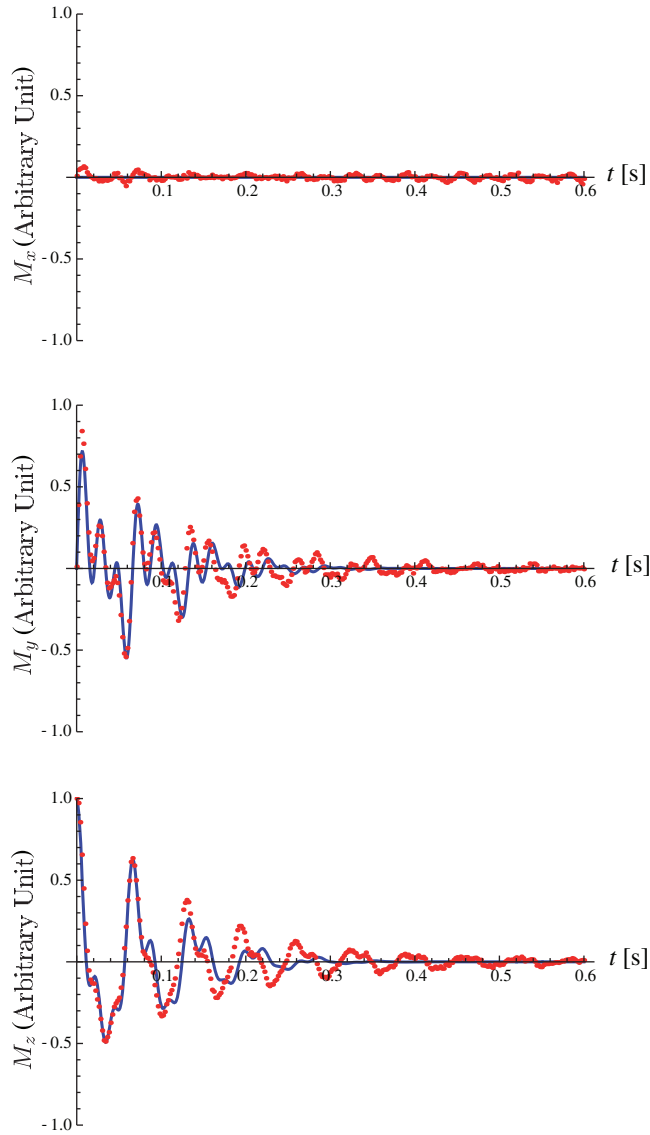


Figure 3. Expectation values M_x , M_y and M_z of spin-1 are shown for case 1, in which all $\omega_{1i}/(2\pi) = 27$ Hz and the initial states of all spins are thermal. Experimental results are shown by dots, and the solid lines are the numerical results, in which known values of coupling constants are employed.

the sole relaxation is not enough to reproduce the decay, as demonstrated by the dashed line in figure 2. Both relaxation and field inhomogeneity must be considered to reproduce the decay rate. We obtain the variance $\sigma/\omega_{1i} = 0.05$ in equation (8) by fitting the data.

3.3. Results

We measure the dynamics of spin-1 in two cases.

In case 1, the initial state is thermal and the transverse fields $\omega_{1i}/(2\pi) = 27$ Hz are applied to all the spins. The expectation values M_x , M_y and M_z of spin-1 are shown in figure 3 as functions of time t . In figure 3, we see that there are structures different from the

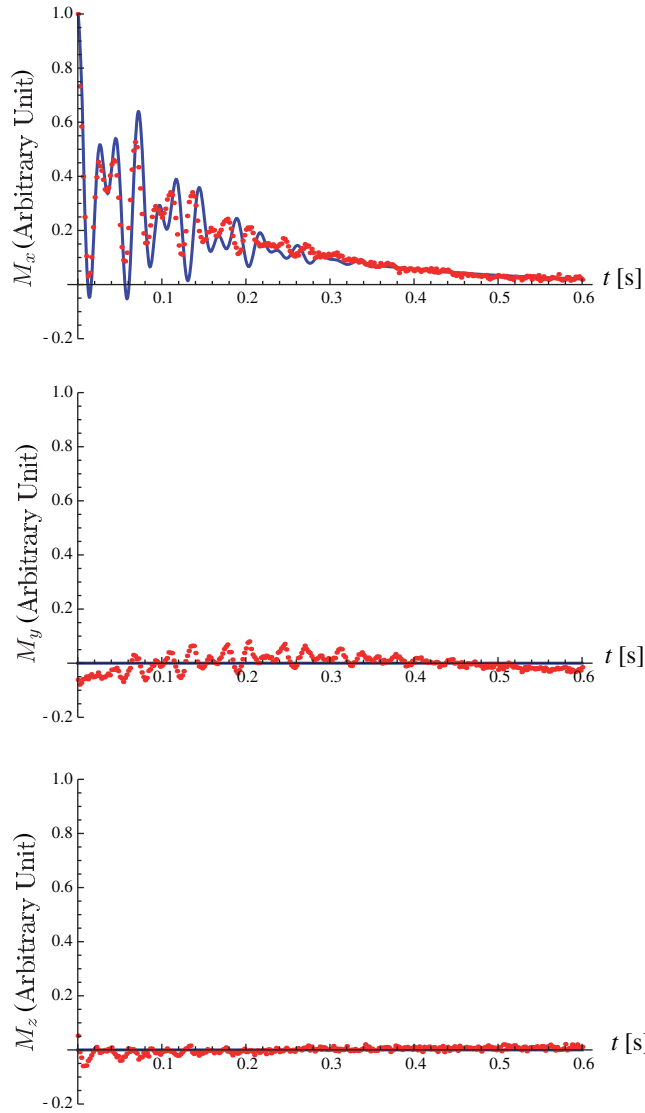


Figure 4. Expectation values M_x , M_y and M_z of spin-1 are shown for case 2, in which $\omega_{11} = 0$ and $\omega_{12}/(2\pi) = \omega_{13}/(2\pi) = 27$ Hz. The initial state of spin-1 is prepared by applying a $\pi/2$ -pulse along the y -axis to the thermal state, while those of spins 2 and 3 remain thermal. Experimental results are shown by dots, and the solid lines show the numerical results, in which known values of coupling constants are used.

simple sinusoidal oscillation, which is expected without interactions. In other words, we obtain information concerning the interactions by measuring spin-1 only. It should be noted, however, that the spin dynamics is affected by relaxations and transverse field inhomogeneities of all spins.

In case 2, we have chosen $\omega_{11} = 0$, $\omega_{12}/(2\pi) = \omega_{13}/(2\pi) = 27$ Hz. Since $\omega_{11} = 0$, we would not expect any dynamics in spin-1 if a thermal state were employed as an initial state. To avoid this problem, the initial state of spin-1 is prepared by applying a $\pi/2$ -pulse along the y -axis to the thermal equilibrium state, while the initial states of spins 2 and 3 remain thermal. We again obtain information on the interactions by measuring only spin-1 as shown in figure 4.

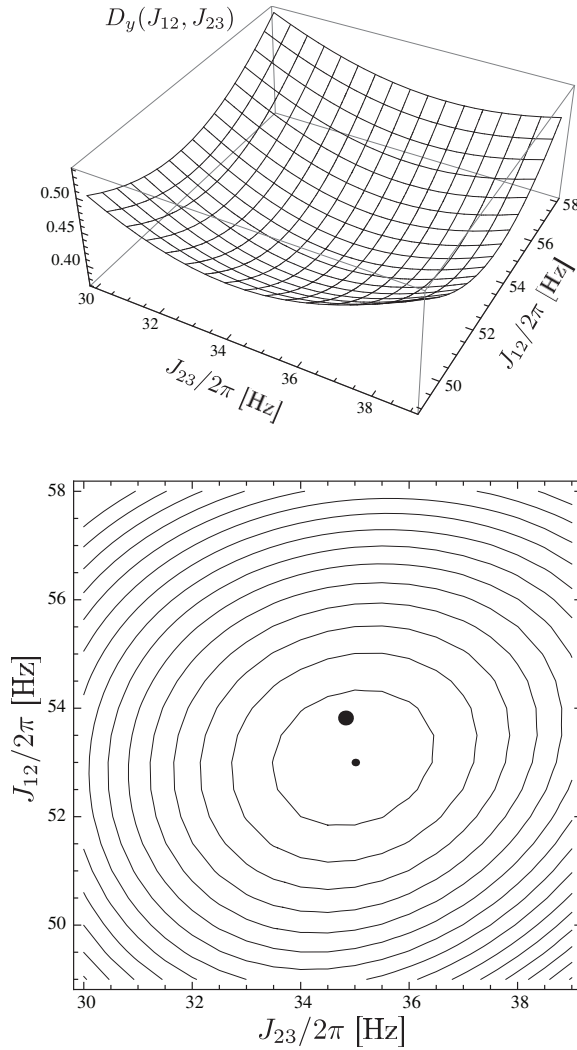


Figure 5. 3D and contour plots of $D_y(J_{12}, J_{23})$ for case 1 when $t_w = 0.05$ s. A clear minimum can be seen. The distance between two neighboring contours in the contour plot is 0.01. The small (big) point shows the estimated (known) values for the coupling constants.

4. Estimation of coupling constants

In this section, we pretend that we do not know the coupling constants J_{12} and J_{23} and, instead, we estimate them by fitting numerically evaluated $\langle I_k^1(t) \rangle$ with various values of (J_{12}, J_{23}) to the experimental data.

Although we previously defined the magnetization $M_k(t)$ of the first spin as the expectation value $\langle I_k^1(t) \rangle$, we temporarily assign $M_k(t)$ to the experimental data and $\langle I_k^1(t) \rangle$ to the corresponding numerical result in order to avoid confusion. Let us define the ‘distance’ between the experimental data $M_k(t)$ and the numerical result $\langle I_k^1(t) \rangle$ by

$$D_k(J_{12}, J_{23}) = \sqrt{\sum_j |\langle I_k^1(t_j, J_{12}, J_{23}) \rangle - M_k(t_j)|^2}.$$

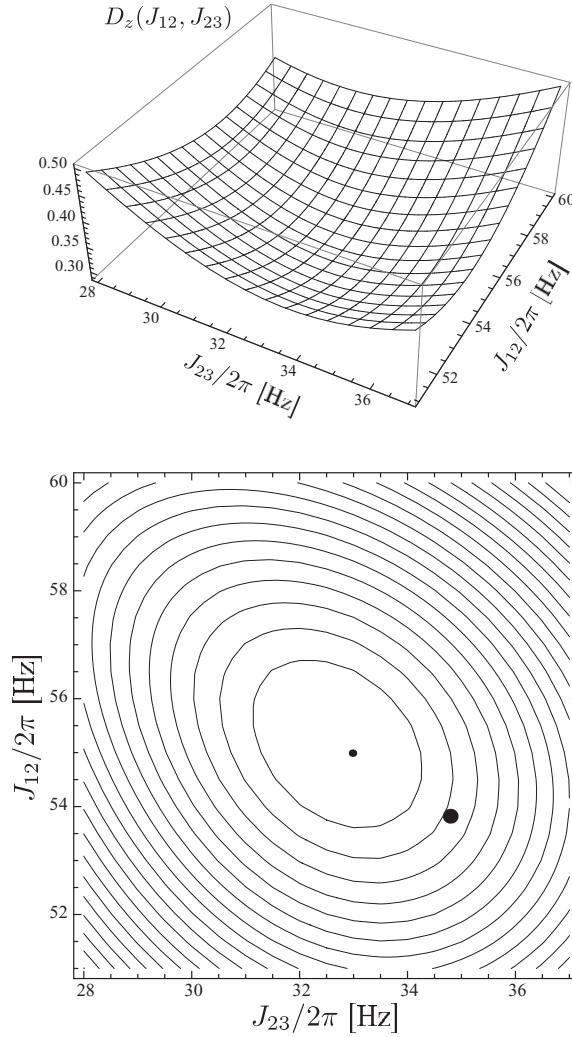


Figure 6. 3D and contour plots of $D_z(J_{12}, J_{23})$ for case 1 when $t_w = 0.05$ s. A clear minimum can be seen. The distance between two neighboring contours in the contour plot is 0.01. The small (big) point shows the estimated (known) values for the coupling constants.

Here $\{t_j\}$ denotes the set of data acquisition points and $\langle I_k^1(t_j, J_{12}, J_{23}) \rangle$ is the numerically evaluated expectation value of the k th component of spin-1 at time t_j with the coupling constants (J_{12}, J_{23}) . In the actual experiment, data were acquired every 0.002 s for $0 \leq t \leq 0.6$ s.

We do not make use of the spectra obtained by the Fourier transforms of time domain signals since the time window is not large enough to provide sharp peaks in the spectra. We can freely select the fitting window from $t = 0$ to $t_w \geq t_0$, where $t_0 = 2\pi/J_{12} + 2\pi/J_{23} \sim 50$ ms is the minimum time required for information to propagate from spin-1 to spin-3 through spin-2 and then propagates back to spin-1. Clearly there is an optimal value for t_w . Too small t_w provides too few data to be fitted and, moreover, the effects of some parameters, such as J_{23} , have no time to influence the dynamics of spin-1, while too large t_w makes relaxations and field inhomogeneities too significant. We estimate the coupling constants with three different values of t_w and compare the results in the following.

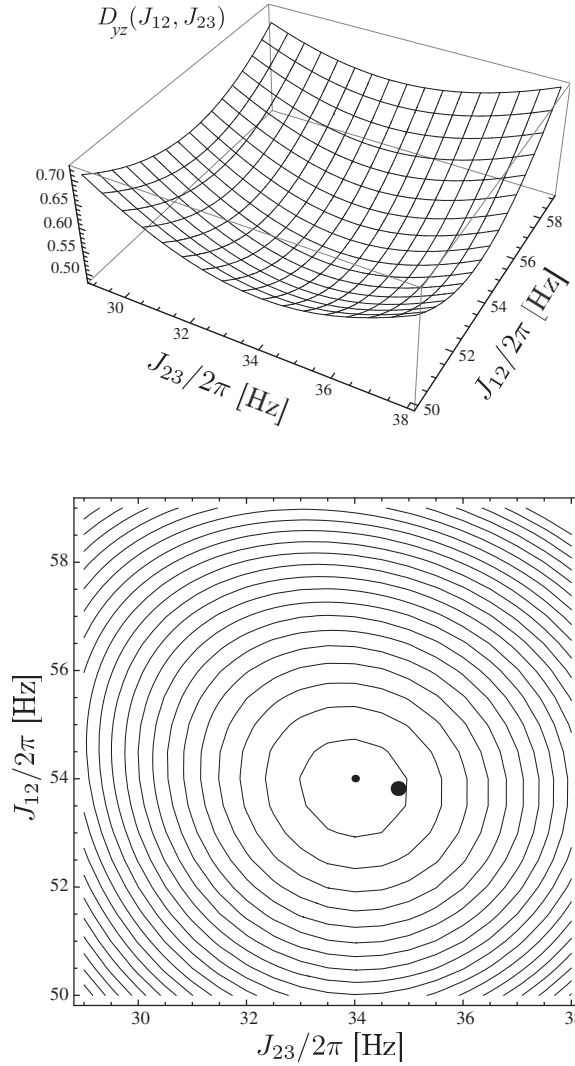


Figure 7. 3D and contour plots of $D_{yz}(J_{12}, J_{23})$ for case 1 when $t_w = 0.05$ s. A clear minimum can be seen. The distance between two neighboring contours in the contour plot is 0.01. The small (big) point shows the estimated (known) values for the coupling constants.

4.1. Case 1: $\omega_{11} \neq 0$

In this case, the initial states of the three spins are prepared in thermal states and transverse fields $\omega_{1i}/(2\pi) = 27$ Hz ($i = 1, 2, 3$) are applied to all three spins.

We find the coupling constants by minimizing $D_y(J_{12}, J_{23})$, $D_z(J_{12}, J_{23})$ or $D_{yz}(J_{12}, J_{23})$ defined as an average of D_y and D_z by

$$D_{yz}(J_{12}, J_{23}) = \sqrt{D_y^2(J_{12}, J_{23}) + D_z^2(J_{12}, J_{23})}.$$

3D and contour plots of the distances $D_y(J_{12}, J_{23})$, $D_z(J_{12}, J_{23})$ and $D_{yz}(J_{12}, J_{23})$ with $t_w = 0.05$ s are shown in figures 5–7, respectively. As expected, clear minima are found in these plots.

Table 1. Estimated coupling constants in case 1 for various window sizes t_w . The values in parentheses are obtained with $T_2(2) = T_2(3) = \infty$.

Case 1	t_w (s)	$J_{12}/2\pi$ (Hz)	$J_{23}/2\pi$ (Hz)
Known values		53.8	34.8
D_y	0.05	53 (52.5)	35 (34.5)
	0.1	55.5 (56)	36 (35)
	0.2	55.5 (55.5)	36.5 (36)
D_z	0.05	55 (54)	33 (32.5)
	0.1	54.5 (54)	30.5 (31)
	0.2	56.5 (53.5)	25.5 (29)
D_{yz}	0.05	54 (53)	34 (33.5)
	0.1	55.5 (55.5)	32 (32)
	0.2	58.5 (58)	24.5 (25)

Table 2. Estimated coupling constants in case 2 for different window sizes t_w . The values in parentheses are obtained with $T_2(2) = T_2(3) = \infty$.

Case 2	t_w (s)	$J_{12}/2\pi$ (Hz)	$J_{23}/2\pi$ (Hz)
Known values		53.8	34.8
D_x	0.05	56.5 (58)	37.5 (38)
	0.1	58 (59)	38 (38.5)
	0.2	59 (61)	38.5 (38)

We obtain the pairs (J_{12}, J_{23}) that minimize $D_y(J_{12}, J_{23})$, $D_z(J_{12}, J_{23})$ and $D_{yz}(J_{12}, J_{23})$, respectively, for $t_w = 0.05, 0.1$ and 0.2 s. The results are summarized in table 1.

4.2. Case 2: $\omega_{11} = 0$

We take $\omega_{11} = 0$ and $\omega_{12}/(2\pi) = \omega_{13}/(2\pi) = 27$ Hz in case 2. To introduce nontrivial spin dynamics into spin-1, a $\pi/2$ -pulse along the y-axis, $Y = \exp(-i\pi I_y^1/2)$, is applied to spin-1 at $t = 0$ after the thermal state has been prepared.

In this case, only D_x is used to estimate the coupling constants, since it is found from figure 4 that no information is obtained from the dynamics of M_y and M_z of spin-1. Figure 8 shows the 3D and contour plots of the distance $D_x(J_{12}, J_{23})$ with $t_w = 0.05$ s. As expected, a unique minimum is found in the figure.

We obtain the pair (J_{12}, J_{23}) that minimizes the distance $D_x(J_{12}, J_{23})$ with different time windows $t_w = 0.05, 0.1$ and 0.2 s. Table 2 summarizes the results.

4.3. Estimation

Regardless of the choice of t_w or (D_x, D_y, D_{yz}, D_z) , the estimated pair (J_{12}, J_{23}) is consistent with each other both in cases 1 and 2. It is clear that the smallest $t_w = 0.05$ s yields the best results when we compare them with the known values of (J_{12}, J_{23}) in [9]. We have also confirmed that a smaller value, $t_w = 0.02$ s, is not large enough to estimate the coupling

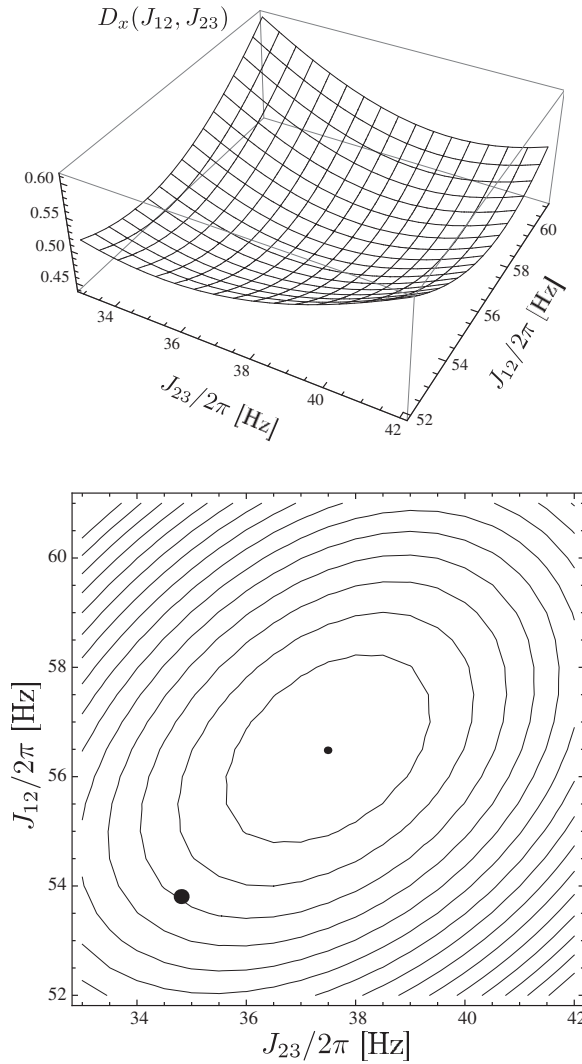


Figure 8. 3D and contour plots of $D_x(J_{12}, J_{23})$ for case 2 with time window $t_w = 0.05$ s. A clear minimum can be seen. The distance between two neighboring contours in the contour plot is 0.01. The small (big) point shows the estimated (known) values for the coupling constants.

constants reliably as shown in figure 9, where the profile has a minimum at $J_{23}/2\pi \sim 0$, which does not correspond to the real value. This behavior clearly shows the significance of the time $t_0 \sim 0.05$ s defined previously. The effect of J_{23} does not manifest itself yet in the behavior of spin-1 for a short time less than t_0 . On the other hand, for $t_w \sim t_0$, relaxation and field inhomogeneity are less serious yet, and the data produce an excellent result, while the results provided by a larger t_w suffer from these effects. So far, as t_w is less than $T_2(2)$ and $T_2(3)$, the effect of these relaxation processes does not affect the dynamics of spin-1 as was claimed in section 2, which justifies our assumption to freely choose $T_2(2)$ and $T_2(3)$. As a result, replacement of $T_2(2)$ and $T_2(3)$ by infinity does not change the dynamics of spin-1 drastically.

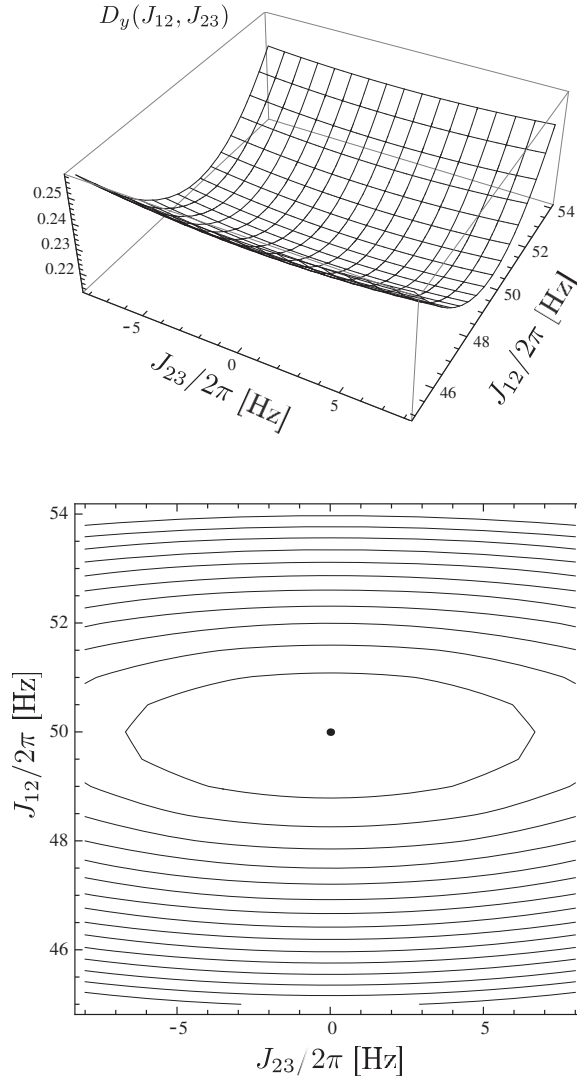


Figure 9. 3D and contour plots of $D_y(J_{12}, J_{23})$ for case 1 with time window $t_w = 0.02$ s. It shows that t_w is not large enough to estimate the coupling constant J_{23} . The distance between two neighboring contours in the contour plot is 0.0028. The point shows the estimated values for the coupling constants.

5. Summary

We have successfully demonstrated that indirect Hamiltonian tomography is possible for a chain of three spins in the NMR setup. As long as the system is small enough for efficient data fitting, the estimated values are surprisingly close to the real ones, even in the presence of a substantial amount of noise and inhomogeneity in the system. This paves the way for the identification of spins and couplings that are off-resonant or would usually be drowned by background noise. Whereas the methods of [5, 8] rely on Fourier analysis, which can only be applied in systems clean enough for sufficiently long time data acquisition, our method can be applied in more noisy cases.

We have shown that there is competition in the observed evolution between the amount of data acquired and the amount of noise coming in. It was found to be optimal to choose rather

short data acquisition times in order to get good agreement between the estimated couplings and their real values.

Acknowledgments

The work of EHL, YK and MN is supported by ‘Open Research Center’ Project for Private Universities: matching fund subsidy from the MEXT (Ministry of Education, Culture, Sports, Science and Technology). YK and MN acknowledge partial support from Grants-in-Aid for Scientific Research from the JSPS (grant no. 23540470). KM acknowledges support from the JSPS Kakenhi (C) (grant no. 22540405). KM and TT are supported in part by Quantum Cybernetics (grant no. 2112004), CREST-JST and FIRST-JSPS (Quantum Information Processing).

References

- [1] Burgarth D, Maruyama K and Nori F 2009 *Phys. Rev. A* **79** 020305
- [2] Burgarth D and Maruyama K 2009 *New J. Phys.* **11** 103019
- [3] Di Franco C, Paternostro M and Kim M S 2009 *Phys. Rev. Lett.* **102** 187203
- [4] Wieśniak M and Markiewicz M 2010 *Phys. Rev. A* **81** 032340
- [5] Burgarth D, Maruyama K and Nori F 2011 *New J. Phys.* **13** 013019
- [6] Shabani A, Kosut R L, Mohseni M, Rabitz H, Broome M A, Almeida M P, Fedrizzi A and White A G 2011 *Phys. Rev. Lett.* **106** 100401
- [7] Shabani A, Mohseni M, Lloyd S, Kosut R L and Rabitz H 2011 *Phys. Rev. A* **84** 012107
- [8] Fasihi M A, Tanaka S, Nakahara M and Kondo Y 2011 *J. Phys. Soc. Japan* **80** 044002
- [9] Kondo Y 2007 *J. Phys. Soc. Japan* **76** 104004
- [10] Nielsen M A and Chuang I L 2000 *Quantum Computation and Quantum Information* (Cambridge: Cambridge University Press)
- [11] Jones J A 2011 *Prog. Nucl. Magn. Reson. Spectrosc.* **59** 91
- [12] Freeman R 1998 *Spin Choreography* (Oxford: Oxford University Press)
- [13] Collins D, Kim K W, Holton W C, Sierzputowska-Gracz H and Stejskal E O 2001 arXiv:quant-ph/0105045
Kim J, Lee J-S, Lee S and Cheong C 2000 *Phys. Rev. A* **62** 022312